Effects of Therapeutic Targeting of Cancer Associated Fibroblasts on Extracellular Matrix Remodeling in an Engineered Tumor Stroma Model

Presented in Partial Fulfillment of the Requirements for Honors Research Distinction in Biomedical Engineering at The Ohio State University

Written by Jonathan Chang | Biomedical Engineering | Submitted: Spring 2018

Jonathan Song | Mechanical and Aerospace Engineering | Faculty Advisor

B. Rita Alevriadou | Biomedical Engineering | Committee Member

Abstract

The tumor microenvironment (TME) is a complex combination of stromal cells and extracellular matrix. The cancer-associated fibroblast (CAF) plays an integral role in remodeling the TME and promoting tumor aggression. In this study, we present a 3D microfluidic model of the tumor stroma, which consists of a single straight micro-channel filled with CAF-embedded or acellular collagen gels. Using this platform, we can quantify both fiber alignment and hydraulic permeability within the collagen matrix. These results provide an enhanced understanding of the CAF's influence on the TME, and this knowledge is critical to the development of more effective cancer treatments. First, this study shows that genetic silencing of phosphatase and tensin homolog (PTEN) in CAFs causes a significant decrease in hydraulic permeability. Moreover, this change occurs without physical reorientation of the collagen fibers, thereby suggesting that PTEN deleted CAFs may be secreting molecules – hypothesized to be hyaluronan – into the TME to cause this observed effect. Using our microsystem as a drug screening platform, we also (1) identify the application of hyaluronidase and the inhibition of p-AKT as promising methods for mitigating the adverse effects of PTEN deletion and (2) show that GDC-0449 undesirably decreases the hydraulic permeability of the TME. Finally, we have also utilized our microsystems to measure the properties of various acellular ECM gel compositions and compared these results to our CAF data. Our findings suggest that HA supplementation to collagen gels does not have an equivalent effect on matrix architecture as CAF-secreted HA. Overall, this study demonstrates the utility of our microfluidic model for studying the TME and provides key insights for developing more effective cancer treatments.

Acknowledgements

First, I would like to thank Dr. Jonathan Song and Alex Avendano for providing me with invaluable guidance throughout the course of this project. Under their mentorship, I developed and grew in my research and critical-thinking abilities. In addition, I would like to acknowledge the entire Microsystems for Mechanobiology and Medicine (MMM) laboratory for the constant feedback and encouragement. Specifically, lab members Aaron Seibel, Christina Ennis, and Amanda Stratton all contributed significantly to the collection and analysis of data that made this project possible. Additionally, I would like to thank Dr. Alevriadou for serving on my thesis defense committee and the Ostrowski lab for their collaboration and provision of materials – including fibroblasts and therapeutics – used in this project.

Finally, I would like to thank the American Cancer Society, American Heart Association, Ohio State Institute for Materials Research, and Pelotonia Junior Investigator Award for their funding to support the MMM lab and this project. I would like to acknowledge the College of Engineering Undergraduate Summer Research Fellowship, STEP, and Pelotonia Undergraduate Fellowship programs whose support allowed me to pursue my research interests.

Table of Contents

Introduction

The Tumor Microenvironment and Cancer-Associated Fibroblasts

Tumors can be considered as complex organs containing numerous highly specialized cell types. In solid tumors, the non-cancer cells and their surrounding extracellular matrix (ECM) combine to form what is known as the tumor microenvironment (TME) – which plays a critical role in regulating disease progression[1]. Often, stromal cell types found in the TME exhibit abnormal behaviors that contribute to cancer aggression[1,2]; the particular cell type focused on in this study is the cancer-associated fibroblast (CAF).

The CAF is one of the most dominant and abundant cell types found in the TME. Normal tissue associated fibroblasts are often charged with the role of secreting ECM to regulate inflammation and the wound-healing process. However, CAFs display an activated state characterized by excessive secretion of ECM components and extreme remodeling of the surrounding environment[2]. Previous studies have illustrated the significance of CAFs in cancer. For instance, *in vitro* experimentation has shown that CAF presence can stimulate the invasion of normally non-invasive cancer cells through Matrigel[3].

Moreover, our collaborators have investigated the effect of phosphatase and tensin homolog (PTEN) – a known tumor suppressor – in CAFs. In their study, cancer cells and CAFs were co-injected into mouse models to stimulate tumor formation. This study showed that CAFs with genetically silenced PTEN expression resulted in increased rates of tumor progression and growth. Furthermore, enhanced ECM and cytokine production was seen in the PTEN deleted CAF condition[4]. Here we further investigate the role of stromal PTEN in regulating cancer progression.

Aberrant Microenvironmental Properties in Cancer

As cancer progresses, the TME is remodeled to exhibit abnormal properties that contribute to the metastatic potency and therapeutic resistance of tumors. Collagen fiber alignment has been identified as a hallmark of many invasive cancers[5]. The oriented fiber structure surrounding tumors has been shown to guide migration and promote intravasation of cancer cells[6]. In an *in vitro* study, fiber alignment was found to increase cancer cell motility through the ECM[7]. In our study, we explore whether CAFs within our microfluidic system reorganize collagen fibers into a more aligned structure.

Additionally, therapeutic resistance in tumors is developed in part by the compression of vasculature. In the TME, matrix components are secreted rapidly and abundantly leading to an increase in solid stress. Consequently, this occurrence leads to the collapse of tumor blood vessels and the reduction of blood flow into the tumor[8]. Hyaluronan or hyaluronic acid (HA) is a glycosaminoglycan whose expression increases as cancer progresses[9]. Due to its high negative charge density, HA can absorb water and swell within the microenvironment. We hypothesize that this swelling will obstruct collagen pores within the TME and lead to decreased hydraulic permeability – the ability for fluid to flow through a porous matrix. For clinical applications, decreased hydraulic permeability may be particularly problematic by lowering drug penetration into the tumor.

Within the TME, collagen fibers can crosslink to form dense fibrotic tissue. During this process, the ECM may stiffen to form a barrier to flow within the tumor; this occurrence is believed to also decrease hydraulic permeability[10] and cause similar problems to what was previously discussed for HA.

Potential Impact and Experimental Motivation

This study works with CAFs taken from patients with pancreatic ductal adenocarcinoma (PDAC) which is one of the most lethal cancer types. PDAC has a 5-year survival rate of less than 5%, and little progress has been made to improve patient outcomes in recent years[11]. Over 90% of new therapeutics fail in clinical trials[9], and many of these failures stem from a poor understanding of the TME. The overall goals of this study are (1) to investigate specific CAF-induced microenvironmental changes that promote cancer aggression and (2) to explore stromal targeted therapies to combat tumor growth.

Specifically, in this study, we design a robust microfluidic model of the TME to study CAF behavior. Techniques for assessing collagen fiber alignment and hydraulic permeability are also presented here. While this project works primarily with PDAC fibroblasts, this platform can be extended for use with all solid tumor types.

Materials and Methods

Building a 3D Microfluidic Model of the Tumor Stroma

The first step in developing our physiological model of the tumor stroma was to fabricate the microfluidic device. The silicon master wafer was created using photolithography, and standard soft lithography techniques were used to mold the micro-devices[12]. This process is illustrated in **Figure 1**. The starting silicon wafer was coated in negative photoresist (SU-8) and selectively exposed to UV light in the specific target geometry. The UV light crosslinked the material and created positive relief features in our desired design. PDMS was then poured over the master, degassed, and cured overnight. The PDMS micro-devices were then cut out, and the ports were created using a 4 mm biopsy punch. To finalize fabrication, the devices were irreversibly sealed to glass slides using plasma treatment. The final device geometry was a single straight channel (L – 5 mm, H – 1 mm, W – 0.5 mm).

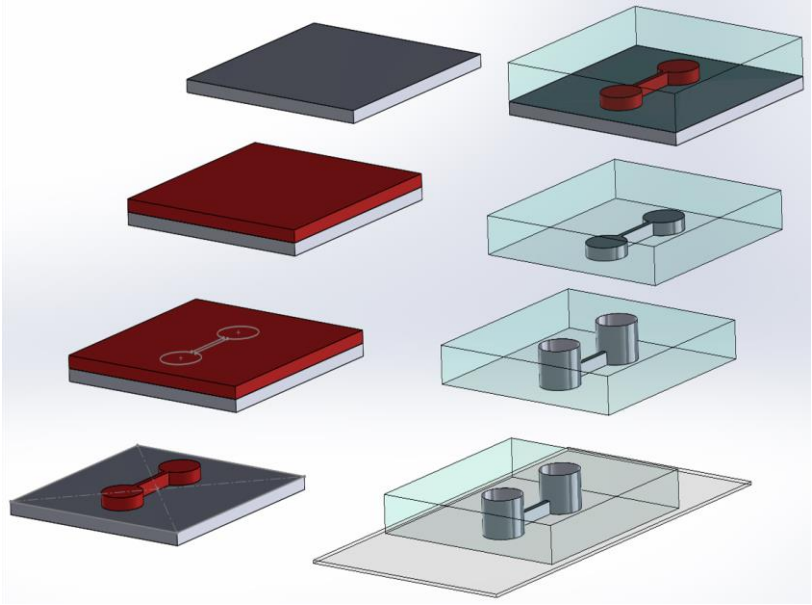

Figure 1: Photo- and soft lithography processes for device fabrication. A silicon master is generated using SU-8 photolithography techniques. PDMS is then poured on the master to create device molds, which are then sealed to a glass slide. Device geometry is a straight channel (L- 5mm, W – 500 µm, H – 1mm) with 4mm inlet and outlet ports.

To complete construction of our tumor stroma model, CAF embedded collagen gels were injected into the PDMS micro-devices. However, prior to injection, each channel was coated with fibronectin (100 µg/ml) for 30 min at 37°C. Following fibronectin treatment, the collagen gel solutions were prepared. Rat tail collagen type I solutions (final concentrations of 6 or 3 mg/ml) were mixed at 4°C with CAF suspended media for a final cell concentration of 1800 cells/µL. These collagen-CAF solutions were injected into the micro-channels and allowed to polymerize at 37°C. This process has been described in further detail previously[13]. Both PTEN deleted (shPTEN) and wildtype (shnc) CAFs were utilized in this project, and these cells – provided by Dr. Mike Ostrowski – were isolated from PDAC patients. PTEN expression was knocked down in these CAFs using shRNA to probe the effect of this genetic ablation. The final tumor stroma model can be seen in **Figure 2**.

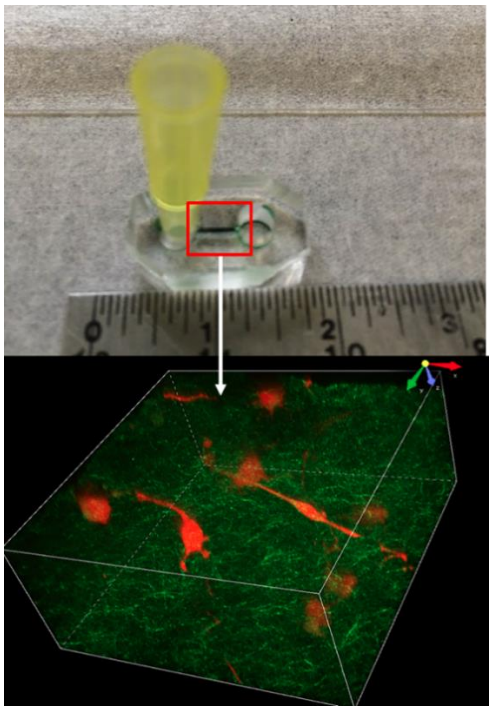

Figure 2: CAF (red) containing 3D collagen (green) gels are injected into the PDMS micro-channel (red square). A pipet tip is inserted into the inlet port to impart a known pressure head for quantification of hydraulic permeability.

Measuring Collagen Fiber Alignment

Collagen fiber alignment was measured using Fast Fourier Transform (FFT) analysis. This technique was originally used to quantify woven fiber orientation in the textile industry[14], but it has recently been exploited for measuring alignment of collagen[15]. The FFT operates by converting image data from the spatial domain to the frequency domain. This transformation

results in a power spectrum being obtained. Next, a radial scan of the power spectrum can be used to obtain a frequency plot of all the collagen fibers in the image. **Figure 3** shows this process.

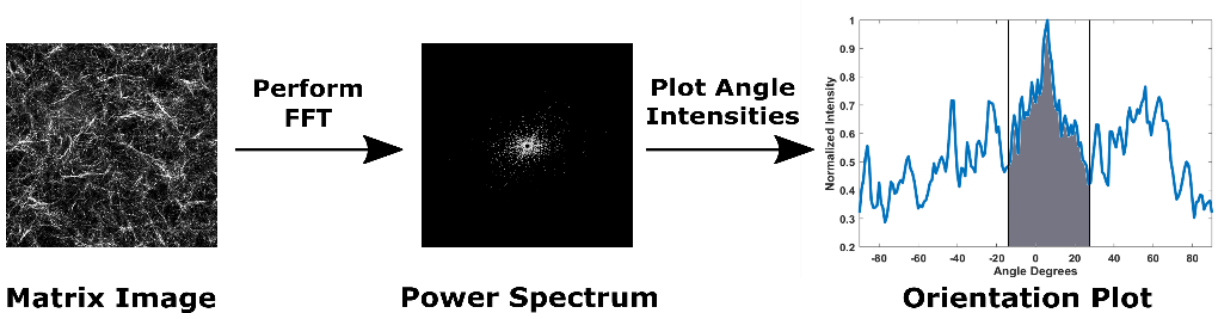

Figure 3: Reflectance microscopy images of collagen fibers are analyzed in MATLAB. The FFT calculation converts the original image to a power spectrum which can be analyzed mathematically. The orientation plot shows the frequency of occurrence for each fiber in the original image. The shaded area of the plot represents the aligned region of the image (± 20 degrees from the dominant angle).

All collagen images were obtained using reflectance microscopy, and the FFT analysis was performed using a MATLAB algorithm. This program was designed to automatically measure fiber alignment for all available image – thus providing our lab with a robust analysis technique. To compare results between samples, an alignment index was measured. This metric is calculated by summing the frequencies in the most aligned region of the image and comparing this sum to the ideally random case as a ratio. Therefore, a value of 1 indicates that the collagen fibers are completely random, and higher alignment indices are indicative of greater alignment.

Quantifying Hydraulic Permeability

To measure hydraulic permeability of our tumor stroma model, a pipet tip was cut (~2 cm) and inserted into the inlet port. This design is shown in **Figure 2**. The pipet tip allowed for the application of a pressure difference across the micro-channel by filling the tip with culture media. Moreover, a rhodamine-bovine serum albumin (rhodamine-BSA) dye was flowed into the micro-device. The movement of this fluorescent dye was tracked using time-lapse microscopy, and after

plotting the dye position over time, the flow speed within the channel was obtained. This process is shown in **Figure 4** below.

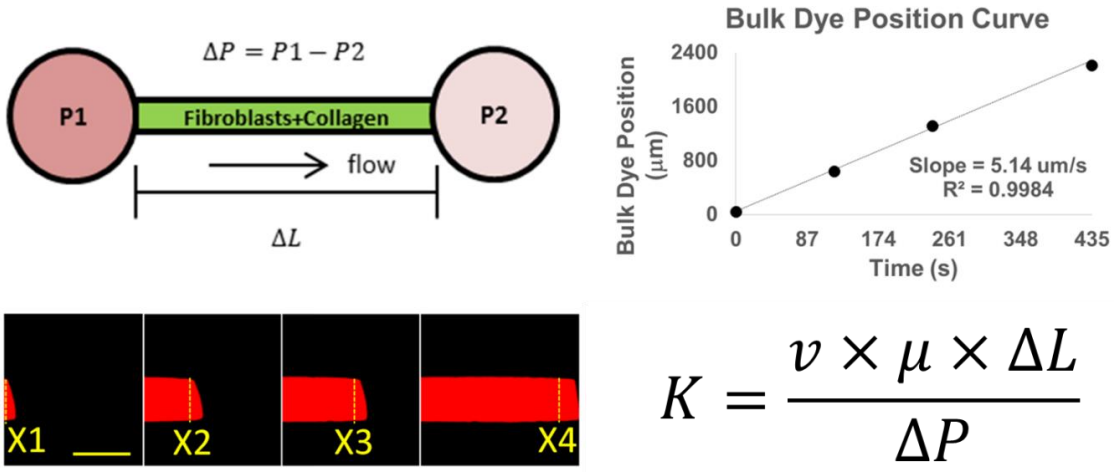

Figure 4: A known pressure difference is applied across the microfluidic channel. This pressure allows fluorescent dye to be flowed across the channel, and the movement can be tracked using time-lapse microscopy. Using the flow speed calculated from these videos, a hydraulic permeability (K) value can be found using Darcy's Law. Modified from Hammer et al.[13]

The flow speed (v) was then used in Darcy's Law to calculate hydraulic permeability. The height of media added to the pipet tip was used to find the applied pressure (P), and the channel length of 5 mm was known for our device. The viscosity (μ) of the cell culture media was assumed to be water. Darcy's Law is also shown in **Figure 4**.

Therapeutic Testing in Microfluidic TME Model

The effect of different therapeutics on TME properties were also tested in our *in vitro* system. Each drug was supplemented into the culture media used to maintain the CAFs in the devices. First, Vismodegib (GDC-0449)[16], a hedgehog pathway inhibitor, was tested. GDC-0449 was supplemented into the cell culture medium at a concentration of 80 μM. Next, an AKT-inhibitor (MK2206) was tested at 4.5 μM. Previous research conducted by our collaborators has shown that PTEN deletion increases activity of p-AKT[4], and we hypothesized that its upregulated occurrence could be contributing to the negative effects observed in the absence of PTEN. Finally, the effect

of hyaluronidase was also tested in our system. Based on our preliminary results, we hypothesized that PTEN deleted CAFs could be secreting excess amounts of hyaluronan into their surrounding TME. By applying hyaluronidase at 0.5 mg/ml, enzymatic degradation of HA was tested as a therapeutic strategy. For all three drug conditions, hydraulic permeability measurements were recorded. This data was collected after 48 hours to allow time for the CAFs to remodel their microenvironment. Moreover, the drug supplemented media was applied to acellular collagen gels as a control, and hydraulic permeability measurements were also performed on these samples.

Acellular Collagen Gel Studies

In addition to our study on CAFs, control experiments with acellular collagen were also performed. Acellular collagen gels were supplemented with HA or a crosslinking agent to test their effects on matrix architecture and hydraulic permeability. To add HA to our collagen gels, a 5 mg/ml stock was diluted with the collagen solution to reach final concentrations of 0.5, 1.0, and 1.5 mg/ml HA. This procedure was done for both 3 and 6 mg/ml collagen solutions. To crosslink the collagen gels, transglutaminase II was added to the collagen gel as 10% of the final volume. These gels were then injected into the micro-channels and maintained for 48 hours before imaging and measuring hydraulic permeability.

Statistical Analysis

For this project, each test was performed on a minimum of three separate instances to ensure repeatability of our experiments and provide sufficient statistical power. All statistical tests were conducted in JMP. Collected data was analyzed using a one-way Analysis of Variance (ANOVA) and Tukey HSD post-testing with an α-level of 0.05.

Results and Discussion

PTEN Deletion Lowers Hydraulic Permeability Without Collagen Fiber Rearrangement

The first experiments performed investigated the effect of PTEN ablation on matrix properties. As previously described, hydraulic permeability measurements were taken in our microfluidic model, and a significant decrease in hydraulic permeability was observed due to PTEN deletion. These results can be seen in **Figure 5**.

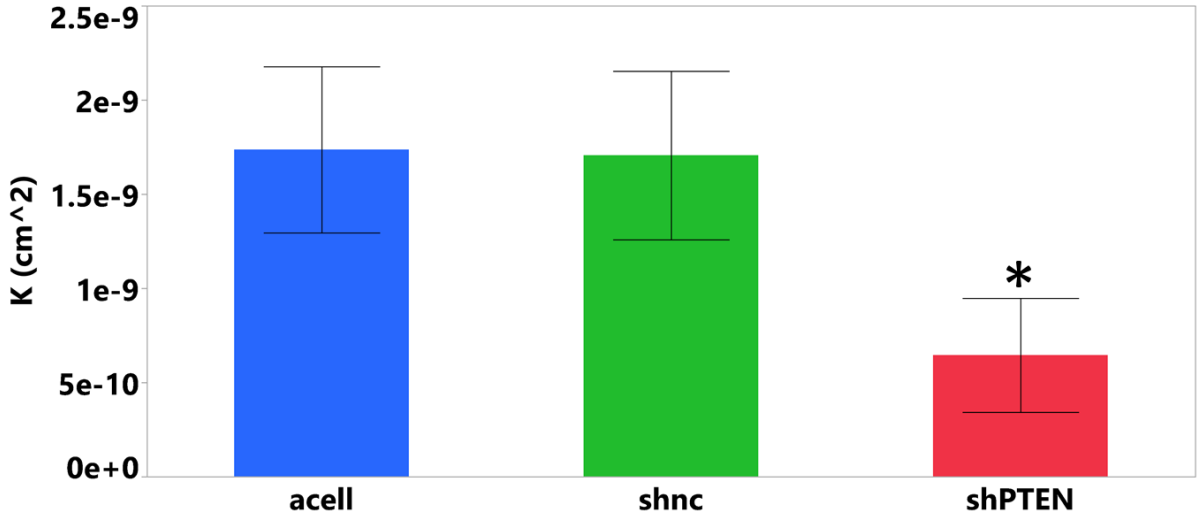

Figure 5: A significant decrease in hydraulic permeability was observed with PTEN deletion. The permeability of the acellular gels was not significantly different than the shnc condition. Error bars represent standard deviations.

This observed result could be a potential mechanism that allows tumors to increase their therapeutic resistance in the absence of PTEN. The lowered permeability of PTEN deleted tumors could lead to poor penetration of anti-tumor agents into tumors. To elucidate the specific microenvironmental changes that cause this decreased permeability, the collagen architecture of these gels was analyzed. We hypothesized that PTEN deleted CAFs would remodel their surrounding environment to have more aligned fibers in comparison to the shnc and acellular conditions.

Reflectance microscopy images were analyzed using FFT to quantify collagen fiber alignment. No significant difference was found between the acellular collagen gel and either CAF condition, which does not support with our initial hypothesis. Within our microfluidic model, the CAFs do not appear to rearrange fibers into an aligned structure. **Figure 6** displays these results.

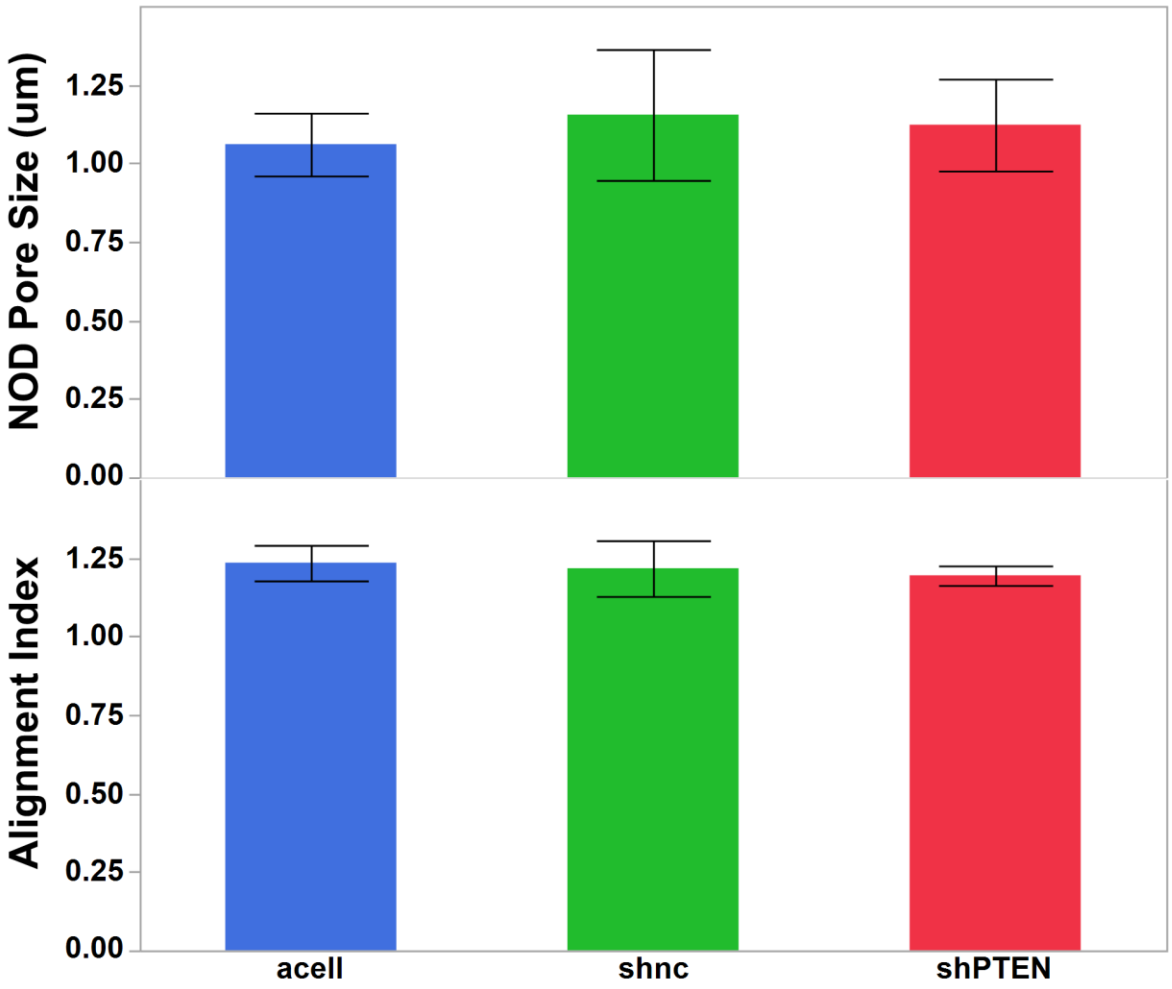

Figure 6: No significant differences in pore size or fiber alignment were seen within our microfluidic TME model.

Moreover, the pore sizes of our collagen images were also analyzed using the nearest-obstacle distance (NOD) technique[17]. Again, no significant difference in pore size (**Figure 6**) was seen between any of the experimental conditions. Combining all results from this portion of the project, shPTEN CAFs appear to lower hydraulic permeability of the TME independent of physical

rearrangement of collagen fibers. Therefore, we then proposed that shPTEN CAFs may lower the permeability of the TME via enhanced secretion of ECM molecules.

Hyaluronidase and MK2206 Recover Decreased Hydraulic Permeability

Two drugs were chosen as potential methods to alleviate the decreased hydraulic permeability seen in the absence of PTEN. Hyaluronidase (HAdase) was chosen as a method to degrade extracellular HA, whereas MK2206 would work intracellularly to inhibit HA production. As previously described, both CAF types were maintained in drug supplemented media, and hydraulic permeability was measured. These results are shown in **Figure 7**.

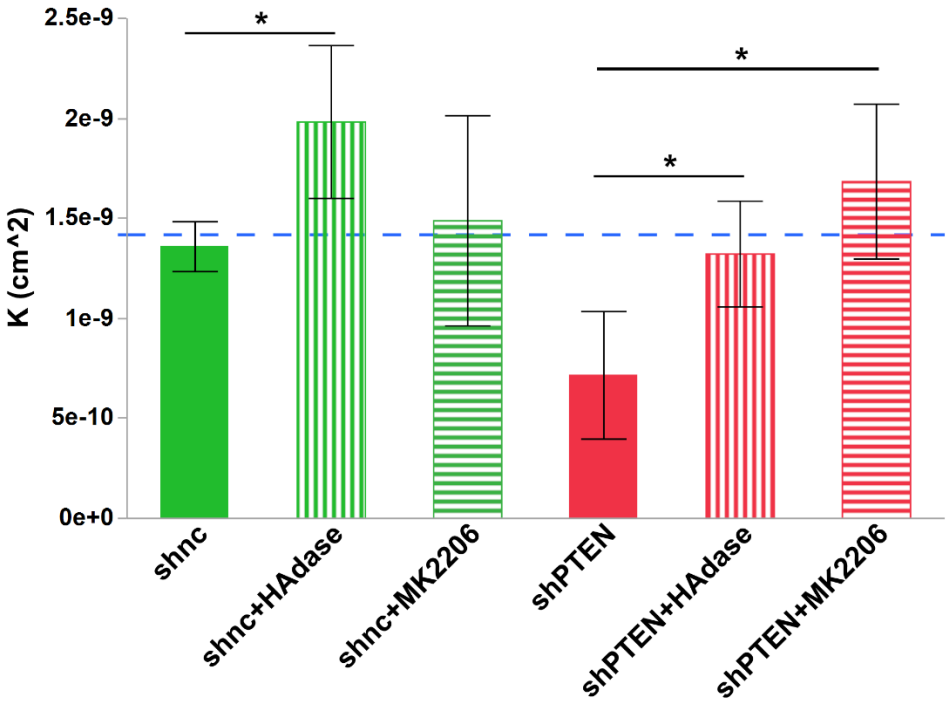

Figure 7: The effect of hyaluronidase and MK2206 on hydraulic permeability was investigated within our microfluidic system. Significant increases in hydraulic permeability were seen for the shPTEN CAFs when the drugs were applied. Acellular gels with both drugs applied were also tested. These controls were not significantly different, and their mean permeability is represented by the blue dotted line.

Both HAdase and MK2206 significantly increased the hydraulic permeability of the shPTEN embedded collagen gels to levels comparable to the acellular controls and shnc gels. In contrast, only application of HAdase had a significant effect on the hydraulic permeability of the

shnc gels; these shnc CAFs are still able to secrete HA which may explain the observed result. Overall, this study shows potential for the use of HAdase and MK2206 to reduce therapeutic resistance in solid tumors where PTEN is diminished in stromal fibroblasts. Used in combination with an anti-tumor agent, these two therapeutics could increase treatment efficacy.

GDC-0449 Lowers Hydraulic Permeability of Wildtype CAFs

In addition to utilizing our microsystem to develop new stromal targeted therapies, this platform can also be used to test the effect of anti-tumor agents on the TME. Our system could identify whether a cancer therapeutic negatively affects the tumor stroma. One drug that we tested was GDC-0449. This therapeutic has been shown by the Ostrowski lab to result in the undesired effect of reducing PTEN expression in CAFs. To test whether this GDC-0449 induced PTEN deletion also negatively affects the physical properties of the TME, we performed hydraulic permeability assays within our system – results shown in **Figure 8**.

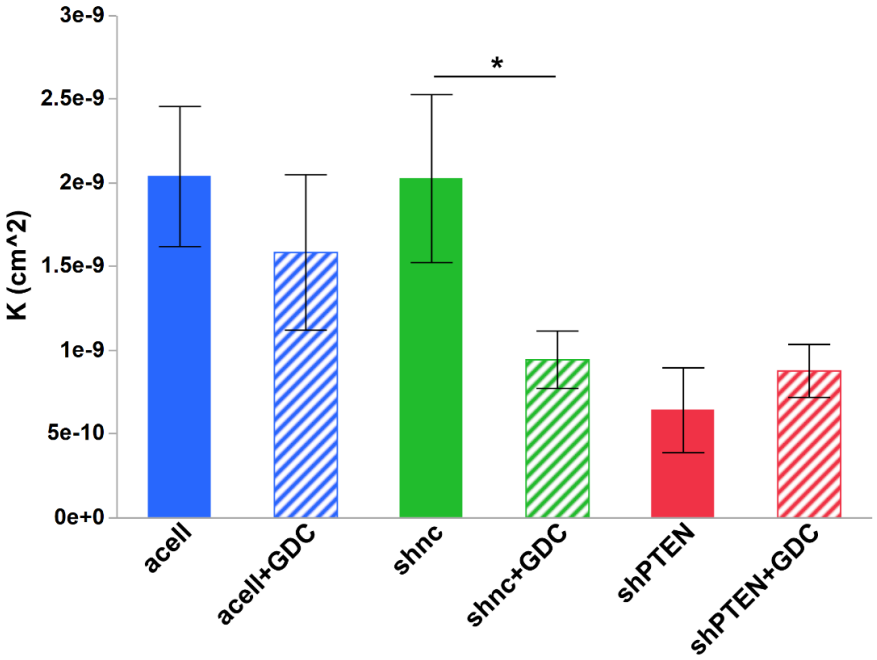

Figure 8: GDC-0449 significantly decreases the hydraulic permeability of shnc embedded collagen gels.

As expected, the application of GDC-0449 to shnc collagen gels caused decreased hydraulic permeability. The shnc+GDC-0449 condition resulted in permeability values comparable to shPTEN. Moreover, the addition of GDC-0449 to the acellular and shPTEN collagen gels did not cause any significant changes.

This reduction in hydraulic permeability after applying GDC-0449 could help to explain why this drug ultimately failed in clinical trials. GDC-0449 appears to negatively affect the properties of the TME by silencing PTEN expression. Furthermore, this result validates our belief that PTEN deletion in CAFs is the cause of decreased hydraulic permeability.

Acellular Collagen Gel Results

Acellular gels were modified via collagen crosslinking and HA addition in this project. These studies were performed to examine whether specific properties of the collagen matrix could be modulated. Pore size and alignment index data is shown in **Figure 9**. As previously stated, 3.0 and 6.0 mg/ml collagen gels were used. Significant increases in pore size were observed for all three HA concentrations at both collagen concentrations. This finding can possibly be explained by the ability for HA to absorb water and swell. The swollen HA could potentially displace the collagen fibers and result in the larger observed pore size. Crosslinking of the collagen gels did not result in statistically significant changes in pore size.

For the fiber alignment results, no significant difference was observed between the 6.0 mg/ml control and the other conditions. However, at 3.0 mg/ml collagen, a significant difference in alignment index was seen between the control and crosslinked condition. One possible explanation for this result is the lower collagen concentration could have reduced steric hindrance to allow the fibers to align more readily.

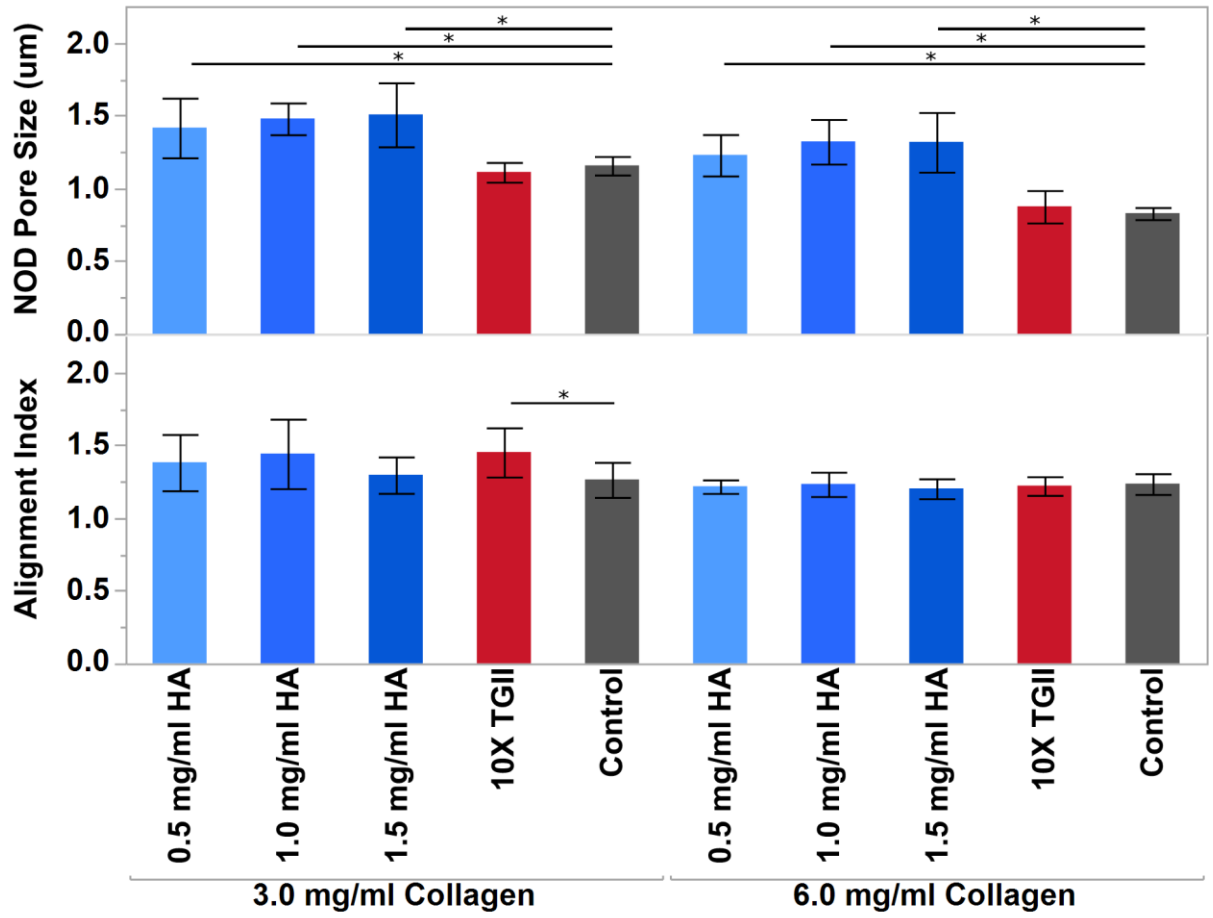

Figure 9: The addition of HA to both 3.0 and 6.0 mg/ml collagen gels causes significant increases in pore size. A significant difference in fiber alignment between the 3.0 mg/ml control and 0.5 mg/ml condition was seen. Error bars represent standard deviation.

Hydraulic permeability measurements were also performed on our acellular gels. **Figure 10** displays these results. Interestingly, the only significant change observed was between the crosslinked and control 3.0 mg/ml collagen gels. The addition of HA did not appear to decrease hydraulic permeability. This finding seems contradictory to our CAF data where the secretion of HA caused decreased permeability. However, the microarchitecture analysis can be used to explain this discrepancy. In our acellular studies, HA addition caused increases in pore size – an effect which is not observed in our cell studies. HA addition and pore size increase may have competing influences on hydraulic permeability in our acellular study. Contrarily, HA secretion

occurs without pore size increase in the CAF study which may allow the changes in hydraulic permeability to be observed.

The findings from this study highlight an important difference between HA supplementation to collagen gels and CAF secreted HA. In other words, simple addition of HA to the collagen gels may not be sufficient in reproducing the high HA content from PTEN deleted CAFs in *in vivo* tumors.

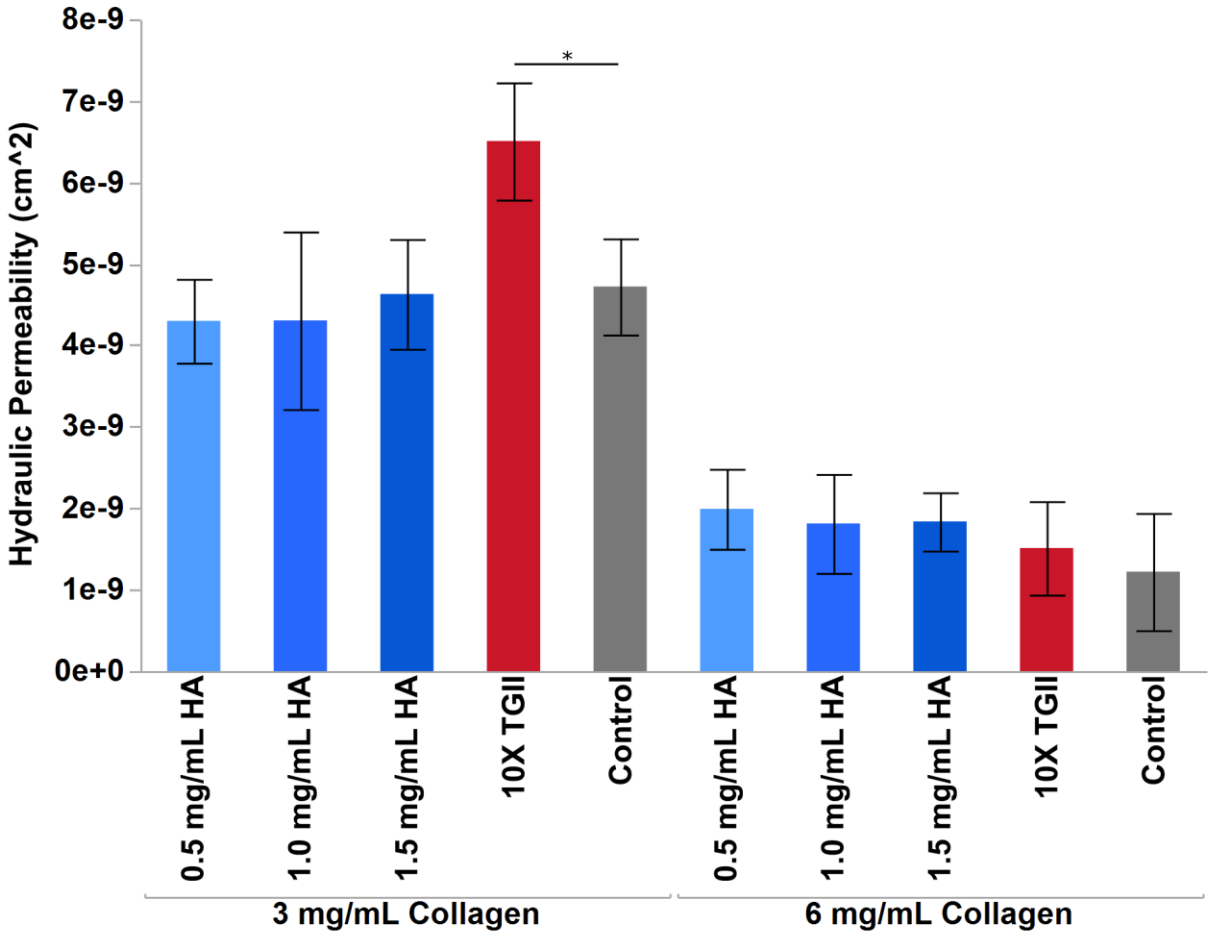

Figure 10: The only significant difference in hydraulic permeability was observed between the crosslinked and control 3.0 mg/ml collagen conditions. HA addition does not appear to affect hydraulic permeability within our acellular gels.

Conclusions and Future Work

Using microfluidic techniques, we have developed a micro-physiological model of the TME. This system – containing CAFs embedded within a collagen hydrogel – allows examination of CAF-mediated changes in matrix properties and the effect of therapeutics on the TME. First, we found that PTEN deletion in CAFs causes significantly decreased hydraulic permeability. This occurrence can be used to explain the increased tumor aggression in the absence of PTEN. In this project, both hyaluronidase and MK2206 have been identified as potential therapeutic approaches to restore the lowered hydraulic permeability in PTEN deleted CAFs. Combined with an anti-tumor agent, these therapies could increase the efficiency of treatment. Moreover, our system has shown that GDC-0449 causes decreases in hydraulic permeability that reproduce the phenotypes observed with PTEN deleted CAFs.

Future studies may begin to investigate the crosstalk that occurs between cancer cells and the TME. The introduction of conditioned media or cancer cells into our system could provide profound insights into the communication present between cancer cells and CAFs. Moreover, we plan to study how additional therapeutics, such as a crosslink inhibitor, affect the properties of the TME.

References

1. Balkwill, F. R., Capasso, M. & Hagemann, T. The tumor microenvironment at a glance. *J. Cell Sci.* **125,** 5591–5596 (2012).
2. Kalluri, R. & Zeisberg, M. Fibroblasts in cancer. *Nat. Rev. Cancer* (2006). doi:10.1038/nrc1877
3. Dimanche-Boitrel, M. T. *et al.* In vivo andin vitro invasiveness of a rat colon-cancer cell line maintaining E-cadherin expression: An enhancing role of tumor-associated myofibroblasts. *Int. J. Cancer* **56,** 512–521 (1994).
4. Trimboli, A. J. *et al.* Pten in stromal fibroblasts suppresses mammary epithelial tumours. *Nature* **461,** 1084–1091 (2009).
5. Gilkes, D. M., Semenza, G. L. & Wirtz, D. Hypoxia and the extracellular matrix: drivers of tumour metastasis. *Nat. Rev. Cancer* (2014). doi:10.1038/nrc3726
6. Han, W. *et al.* Oriented collagen fibers direct tumor cell intravasation. *Proc. Natl. Acad. Sci. U. S. A.* **113,** 11208–11213 (2016).
7. Fraley, S. I. *et al.* Three-dimensional matrix fiber alignment modulates cell migration and MT1-MMP utility by spatially and temporally directing protrusions. *Sci. Rep.* (2015). doi:10.1038/srep14580
8. Rahbari, N. N. *et al.* Anti-VEGF therapy induces ECM remodeling and mechanical barriers to therapy in colorectal cancer liver metastases. *Sci. Transl. Med.* (2016). doi:10.1126/scitranslmed.aaf5219
9. Provenzano, P. P. *et al.* Enzymatic Targeting of the Stroma Ablates Physical Barriers to Treatment of Pancreatic Ductal Adenocarcinoma. *Cancer Cell* (2012). doi:10.1016/j.ccr.2012.01.007
10. Jain, R. K., Martin, J. D. & Stylianopoulos, T. The Role of Mechanical Forces in Tumor Growth and Therapy. *Annu. Rev. Biomed. Eng.* (2014). doi:10.1146/annurev-bioeng-071813-105259
11. Hidalgo, M. Pancreatic Cancer. *N. Engl. J. Med.* **362,** 1605–1617 (2010).
12. Dong, Q., Xia, Y. & Whitesides, G. Soft lithography for micro- and nanoscale patterning. *Nat. Protoc.* **5,** 491–502 (2010).
13. Hammer, A. M. *et al.* Stromal PDGFR-α Activation Enhances Matrix Stiffness, Impedes Mammary Ductal Development, and Accelerates Tumor Growth. *Neoplasia (United States)* **19,** 496–508 (2017).
14. Pourdeyhimi, B. & Dent, R. Measuring Fiber Orientation in Nonwovens Part IV: Flow Field Analysis. *Text. Res. J.* **67,** 181–187 (1997).
15. Ng, C. P., Hinz, B. & Swartz, M. A. Interstitial fluid flow induces myofibroblast differentiation and collagen alignment in vitro. *J. Cell Sci.* (2005). doi:10.1242/jcs.02605
16. Kim, E. J. *et al.* Pilot Clinical Trial of Hedgehog Pathway Inhibitor GDC-0449 (Vismodegib) in Combination with Gemcitabine in Patients with Metastatic Pancreatic Adenocarcinoma. *Clin. Cancer Res.* **20,** 5937–5945 (2014).
17. Lang, N. R. *et al.* Estimating the 3D pore size distribution of biopolymer networks from directionally biased data. *Biophys. J.* **105,** 1967–75 (2013).